

## Reconfigurable bandstop to allpass filter using defected ground structure in K-band for millimeter-wave communications

Adib Othman<sup>1,2</sup>, Noor Azwan Shairi<sup>2</sup>, Huda A. Majid<sup>1</sup>, Zahriladha Zakaria<sup>2</sup>, Imran Mohd Ibrahim<sup>2</sup>, Mohd Haizal Jamaluddin<sup>3</sup>, Anwar Faizd Osman<sup>4</sup>

<sup>1</sup>Faculty of Engineering Technology, Universiti Tun Hussein Onn Malaysia (UTHM), Parit Raja, Malaysia

<sup>2</sup>Centre for Telecommunication Research & Innovation (CeTRI), Fakulti Kejuruteraan Elektronik dan Kejuruteraan Komputer, Universiti Teknikal Malaysia Melaka (UTeM), Melaka, Malaysia

<sup>3</sup>Wireless Communication Centre, Faculty of Electrical Engineering, Universiti Teknologi Malaysia (UTM), Johor Bahru, Malaysia

<sup>4</sup>Rohde & Schwarz Malaysia Sdn. Bhd., Shah Alam, Selangor, Malaysia

### Article Info

#### Article history:

Received Feb 28, 2022

Revised Jul 1, 2022

Accepted Jul 26, 2022

#### Keywords:

Bandstop to allpass

Defected ground structure

Millimeter-wave

PIN diode

Reconfigurable filter

### ABSTRACT

In this paper, a reconfigurable bandstop to allpass filters using defected ground structure (DGS) in K-Band for millimeter-wave communications is proposed. Mathematical analysis of the DGS is discussed in this paper for the bandstop and allpass responses. The reconfigurable filter is performed by using an ideal switch with open circuit and short circuit conditions on DGS at several locations. Hence, two filter designs with different DGS are investigated for their performance in both simulation and measurement. As a result, the ideal switch at location S3 gives the best performance for both DGSs with a narrowband bandstop response and a wideband allpass response with insertion loss of less than 1 dB and return loss of more than 10 dB at the 26 GHz band. Hence, the proposed reconfigurable filter is suitable for millimeter-wave front-end communications.

*This is an open access article under the [CC BY-SA](https://creativecommons.org/licenses/by-sa/4.0/) license.*



### Corresponding Author:

Noor Azwan Shairi

Centre for Telecommunication Research & Innovation (CeTRI)

Fakulti Kejuruteraan Elektronik dan Kejuruteraan Komputer, Universiti Teknikal Malaysia Melaka

Hang Tuah Jaya, 76100, Durian Tunggal, Melaka, Malaysia

Email: noorazwan@utem.edu.my

## 1. INTRODUCTION

Complex and dynamic wireless communication systems have resulted from the demand for increasing data rates and the allocation of a spectrum band at higher frequencies. This can be seen in the implementation of a new fifth-generation (5G) technology in millimeter-wave frequency bands [1]. However, this new implementation will interfere with the existing technology as reported in [2], where the simulation results show that the fixed-satellite service (FSS) satellite receives interference from many IMT-2020s (5G communication standard) in the millimeter-wave (mm-wave) band. Therefore, a cognitive radio (CR) is needed in 5G millimeter-wave communications to minimize any possible interference. Hence, there are several solutions on the interference mitigation techniques in CR systems, such as spectrum sensing algorithms based on energy detection [3], cooperative spectrum sensing for reducing the interference and increasing the utilization of the unused frequency spectrum [4], multi-hop multiple input multiple output (MIMO) decode-and-forward relaying protocol [5], interference management techniques for device-to-device (D2D) applications [6] and ultra-wideband (UWB) receiver architecture with interference mitigation that exploits the spatial and spectral diversity for high speed multi-user communication [7]. Besides, in front-end systems of CR, there is a need for reconfigurable devices such as filters [8] and antennas [9] to allow multi-channel, multi-band and multi-functional operations, and thus, at the same time, provide an interference

mitigation solution. This is known as an active interference cancellation to physically suppress interference in the front-end receiver [7]. Therefore, proper circuit or device control using PIN or varactor diodes is very important, as discussed in [8] and [9].

Islam *et al.* [8], switchable filters are one of the reconfigurable filter techniques that can be used in a CR system. Under this technique, filter mode transformation can be performed between bandpass to bandstop [10]–[14] and bandstop to allpass [15]–[19]. By looking at the bandstop to allpass filter mode transformation, there are different resonators used in the switchable filter design, such as cascaded substrate integrated waveguide (SIW) resonators [15], lumped-element resonators [16], stepped impedance resonators [17], evanescent-mode cavity resonators [18], and microstrip line resonators [19].

From literatures, defected ground structure (DGS) is used in RF and microwave circuit designs such as antennas [20], [21], filters [22], [23], power amplifiers [24] and power dividers [25]. The use of the DGS in these circuits has different purposes, such as harmonics or frequency suppression [20], [22], [23], [25], wideband performance [21], circuit miniaturization [22], [23], [25] and load matching network [24]. Therefore, in this paper, a DGS is proposed for the reconfigurable bandstop to allpass filter for mm-wave communications such as 5G technology in the 26 or 28 GHz band (K-band). Two different DGSs in [26] and [27] are investigated and redesigned to be switchable filters between bandstop and allpass responses. Besides, a mathematical analysis is presented and discussed in this paper for the switching between bandstop and allpass responses. The proposed designs can be used in in front-end systems of CR systems or in switch designs [28], [29] for 5G millimeter-wave communications.

**2. MATHEMATICAL ANALYSIS OF RECONFIGURABLE DGS MODEL**

This section discusses a reconfigurable DGS model by referring to a mathematical analysis. The analysis is based on two conditions which are bandstop dan allpass responses. Figure 1 shows an equivalent circuit of the reconfigurable DGS whereby a PIN diode (ideal switch) is used as a switching element between bandstop and allpass responses.

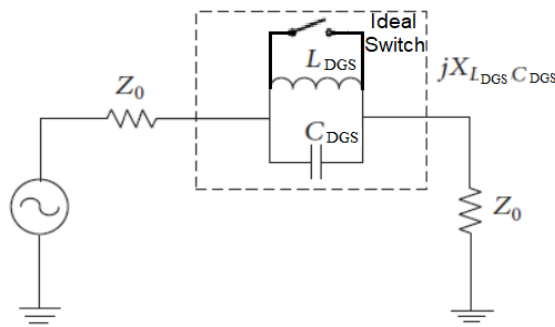


Figure 1. Equivalent circuit model of reconfigurable DGS

A simple parallel  $L$  and  $C$  is the equivalent circuit of DGS as reported in [30]. Therefore, the impedance of DGS is given as (1).

$$\begin{aligned}
 Z_{DGS} &= jX_{LC} \\
 &= \frac{(\frac{1}{j\omega C})(j\omega L)}{(\frac{1}{j\omega C})+(j\omega L)} = \frac{j\omega L}{1+ \omega^2 LC} .
 \end{aligned}
 \tag{1}$$

Now consider the OFF state of the PIN diode, where ideally it will be an open circuited of the DGS. Thus, the DGS responses as a bandstop. Then, the transmission matrix ( $ABCD$ ) of the DGS is (2).

$$T_{DGS} = \begin{bmatrix} 1 & Z_{DGS} \\ 0 & 1 \end{bmatrix} = \begin{bmatrix} 1 & \left( \frac{j\omega L}{1+ \omega^2 LC} \right) \\ 0 & 1 \end{bmatrix} .
 \tag{2}$$

From (2), by using conversion between  $ABCD$  to  $S$ -parameter, the bandstop response of  $S_{21}$  is derived as (3):

$$S_{21} = \frac{2}{A + \frac{B}{Z_0} + Z_0 C + D} = \frac{2}{2 + \frac{j\omega L}{(1 - \omega^2 LC)Z_0} + Z_0} \tag{3}$$

where  $Z_0$  is the characteristic impedance of the transmission line of the DGS. It can be seen that from (3), if  $Z_0=1$ , which is a normalized impedance, the notch of the bandstop is due to the  $L$  and  $C$  components. Then, the resonant frequency of the DGS can be determined when;

$$j\omega L - \frac{j}{\omega C} = 0 . \tag{4}$$

Thus,

$$f_0 = \frac{1}{2\pi LC} \tag{5}$$

where  $f_0$  is the resonant frequency in Hertz.

The next analysis is considering an ON state of the PIN diode where ideally it will be a short circuited of the DGS. Thus, the DGS responses as an allpass. Referring to [30], the rectangular parts of the dumbbell DGS increase the route length of current and the effective inductance. Meanwhile, the slot part accumulates charge and increases the effective capacitor of the microstrip line. Therefore, theoretically, the allpass response can be obtained if at least one or both of the components of  $L$  and  $C$  are zero. Considering the case where the rectangular parts of DGS are short circuited by the ON state of the PIN diode, thus  $L$  is zero and let  $Z_0 = 1$ , which is a normalized impedance, then,  $S_{21}$  of (3) becomes (4);

$$S_{21} = \frac{2}{2 + \frac{j\omega(0)}{(1 - \omega^2(0)C) + 1}} = \frac{2}{3} \approx 1 \tag{6}$$

or in decibel in (7).

$$|S_{21}|^2 dB = 20 \log_{10}(1) = 0 \text{ dB} . \tag{7}$$

From (7), it can be seen that an ideal zero insertion loss can be achieved, where an allpass response is produced. Based on the mathematical analyses, further investigation in any electronic design automation (EDA) software (for example, CST software) needs to be carried out for any type of DGS in order to make it switchable between bandstop and allpass responses. Different types of DGS have different locations of the effective capacitance and inductance that could be put into one or more PIN diodes for the switching operation.

### 3. RECONFIGURABLE DGS DESIGNS

#### 3.1. DGS designs

The concept of an ideal switch is used to produce the reconfigurable DGS design. Each DGS is presented by two layouts, which are open circuit condition (active DGS) and short circuit condition (inactive DGS). Uneven U-shape Dumbbell layout DGS as shown in Figure 2. Figure 2(a) shows the Uneven U-shape Dumbbell from [26], which is ideally in open circuit condition. Then, a short circuit conductor is applied to the DGS as shown in Figure 2(b) and becomes a short circuit condition. The same holds true for the T-shape Loaded DGS from as shown in Figure 3 [27] as shown in Figure 3(a) and Figure 3(b) respectively. A summary of their dimensions is shown in Table 1.

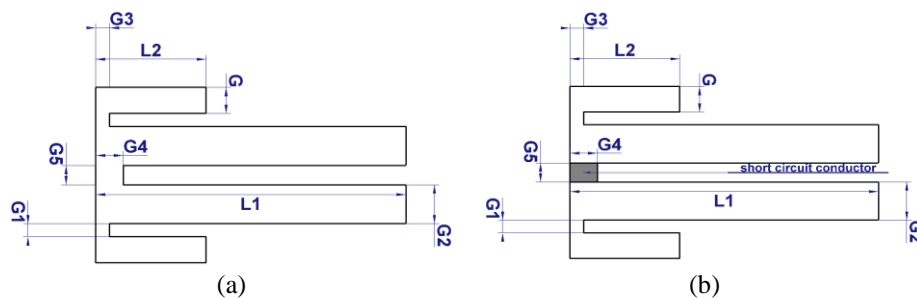


Figure 2. Uneven U-shape Dumbbell layout DGS, (a) active DGS and (b) inactive DGS

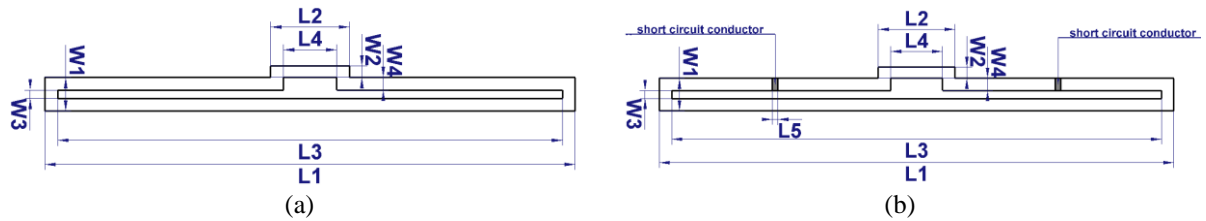


Figure 3. T-shape Loaded layout DGS, (a) active DGS and (b) inactive DGS

Table 1. Uneven U-shape Dumbbell and T-shape Loaded DGS dimensions

Uneven U-shape Dumbbell		T-shape Loaded	
Parameter	Dimension (mm)	Parameter	Dimension (mm)
L1	2.25	L1	14.03
L2	0.80	L2	2.09
G	0.20	L3	13.35
G1	0.10	L4	1.41
G2	0.30	L5	0.15
G3	0.10	W1	0.89
G4	0.20	W2	0.34
G5	0.15	W3	0.22
		W4	0.34

**3.2. The ideal switch locations on DGS for allpass response**

To implement the best position for the ideal switch, the switch in short circuit condition is placed in three different locations for both DGSs to get the best performance of allpass responses for the switchable filter. These different locations have the effect of altering the propagation of EM waves and radiation characteristics and hence produce different responses for S-parameters shown in Figure 4. Figure 4(a), Figure 4(b) and Figure 4(c) show the S1, S2 and S3 locations of the short circuit ideal switch on the Uneven U-shape Dumbbell DGS. The same labelling is also applied on T-shape Loaded DGS as shown in Figure 5, Figure 5(a), Figure 5(b) and Figure 5(c) respectively.

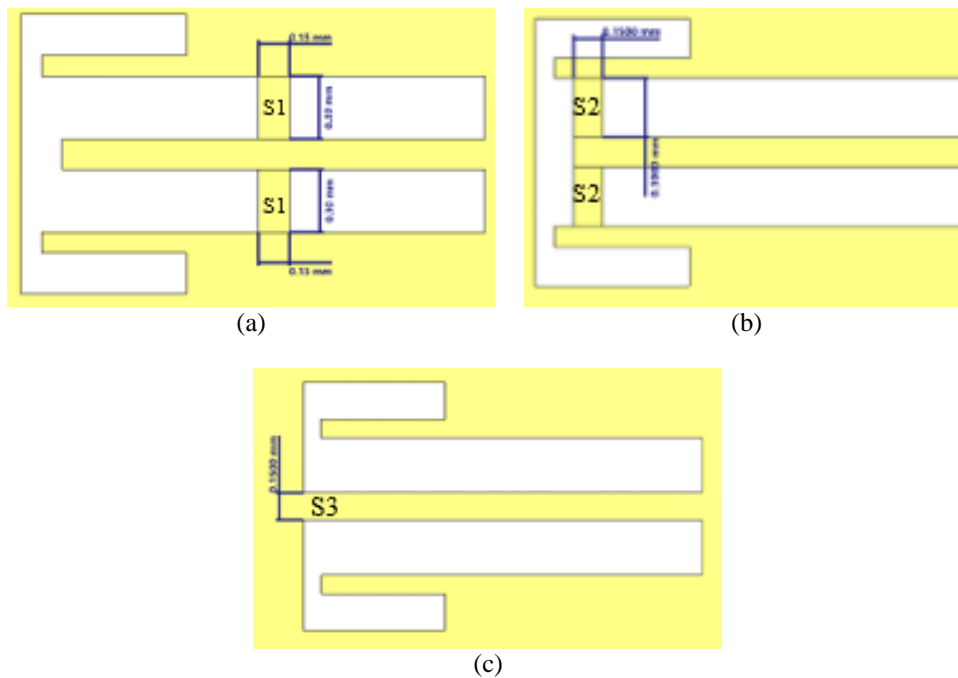


Figure 4. Short circuit ideal switches placement on Uneven U-shape Dumbbell DGS, (a) S1, (b) S2 and (c) S3 locations

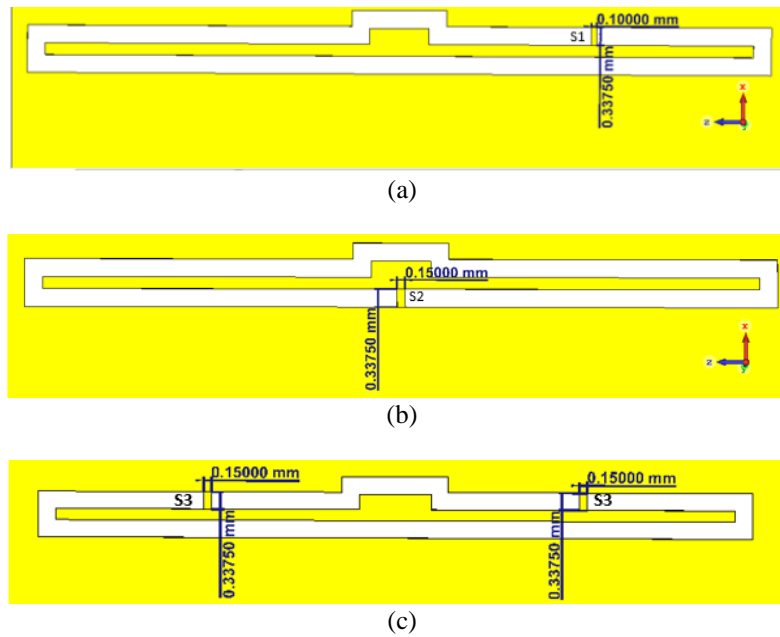


Figure 5. Short circuit ideal switches placement on T-shape Loaded DGS, (a) S1, (b) S2, and (c) S3 locations

### 3.3. DGS prototypes

Prototype of ideal switchable DGS filters as shown in Figure 6. Figure 6(a) and Figure 6(b) show the top and bottom views of an ideal switchable DGS filter prototype made with the Uneven U-shape Dumbbell and the T-shape Loaded layouts respectively. All filters were fabricated on a Rogers RT/Duroid 5880 substrate with a 0.254 mm thickness and a relative dielectric constant,  $\epsilon_r$  of 2.2. The prototypes were measured using the N5234B PNA-L Microwave Network Analyzer. The network analyzer, with the combination of high precision cables, was used to measure insertion loss and return loss of the prototypes and validated with simulation results.

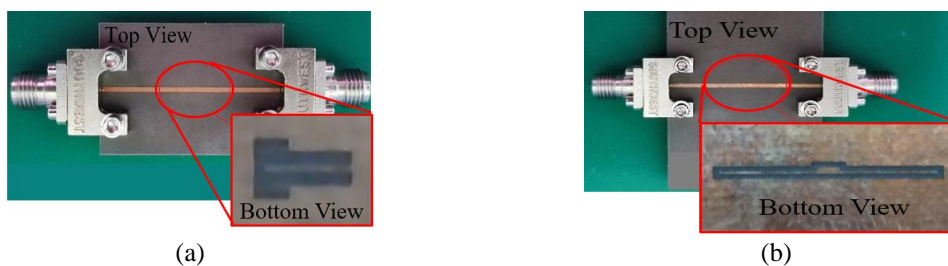


Figure 6. Prototype of ideal switchable DGS filters, (a) with Uneven U-shape Dumbbell DGS and (b) with T-shape Loaded DGS

## 4. RESULTS AND DISCUSSION

Figure 7 shows simulation results of an ideal switchable DGS filter using the Uneven U-shape Dumbbell with locations S1, S2 and S3 as discussed in Section 3. It is clearly shown as the ideal switch moves towards the slot of the dumbbell (from S1 to S3), the insertion loss and return loss become better with a wider bandwidth of allpass response and the bandstop resonance magnitude at higher frequency was reduced to help produce a better wideband allpass response. As a result, the S3 location shows the best result compared to S1 and S2.

Figure 8 shows simulation results of the ideal switchable DGS filter using the T-shape Loaded layout with locations S1, S2 and S3 as discussed in Section 3. Although it showed a wideband allpass response, S1 location does not offer good return loss. This is due to S1 location produce the asymmetrical structure for the DGS. The S2 location has slightly improved the return loss result in the 26 GHz band but

does not offer wideband allpass response. This is due to S2 location does not produce enough short circuit conditions to decouple the DGS effect, which can be seen by the appearance of bandstop resonance at 25.5 GHz. Lastly, the S3 location gave the best wide bandwidth of allpass response with insertion loss of approximately at 1 dB and return loss below 10 dB in the 26 GHz band. Table 2 summarizes the insertion loss and return loss performances for both types of DGS.

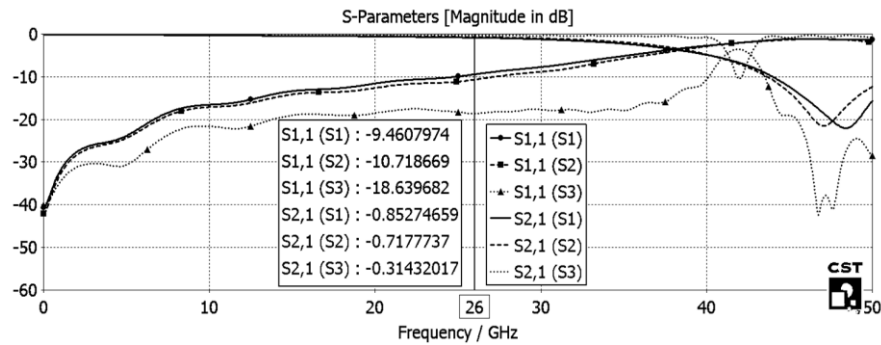


Figure 7. Simulation results of return loss (S11) and insertion loss (S21) of the ideal switchable DGS filter using Uneven U-shape Dumbbell layout in the short circuit condition with S1, S2 and S3

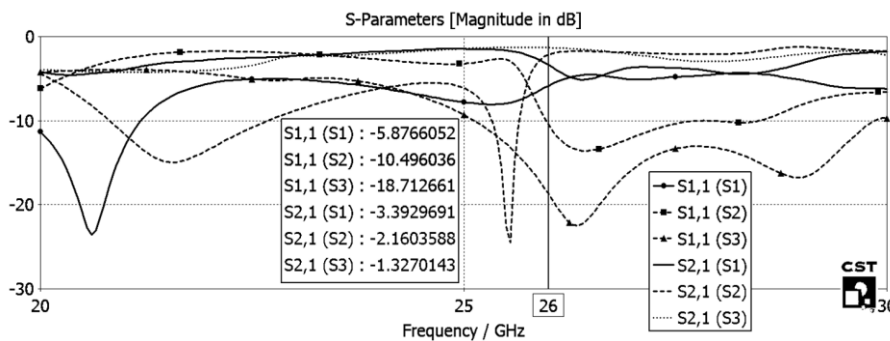


Figure 8. Simulation results of return loss (S11) and insertion loss (S21) of the ideal switchable DGS filter using T-shape Loaded layout in the short circuit condition with S1, S2 and S3 locations

According to Table 2, the ideal switch location on S3 gave the best result in insertion loss and return loss for both DGS layouts compared to S1 and S2 locations. Furthermore, the S3 location manages to decouple both the transmission line and the DGS and hence let the EM waves pass to the output port. This phenomenon is theoretically the same as short circuiting the inductance and capacitance of DGS as shown in mathematical modelling and the DGS equivalent circuit as discussed in Section 2. As a result, DGS layouts with the ideal switch location on S3 were chosen as fabricated prototypes for validation.

Table 2. Return loss and Insertion Loss performance at 26 GHz

Ideal Switch Location	Uneven U-shape Dumbbell		T-shape Loaded	
	Insertion Loss (S21 in dB)	Return Loss (S11 in dB)	Insertion Loss (S21 in dB)	Return Loss (S11 in dB)
S1	0.85	9.46	3.39	5.88
S2	0.72	10.72	2.16	10.50
S3	0.31	18.64	1.33	18.71

Figure 9 shows simulation and measurement results of ideal switchable DGS filter using the Uneven U-shape Dumbbell. It can be observed that the open circuit condition filter with the bandwidth of attenuation response was approximately 1.65 GHz at 10 dB level and a more compact DGS circuit size than compared to in [26]. The narrow bandwidth result with high attenuation magnitude has the potential to aid in improving

the frequency selectivity of the filter significantly. Meanwhile, a short circuit condition has nullified the DGS effect of the filter and hence produces a wideband allpass response with an insertion loss of approximately 1 dB and a return loss of less than 10 dB. As a whole, the simulation and measurement results are slightly different because of the tolerance in the fabrication process. Some of the measurements have ripple effects that might be from a loose connection between connectors and cables during the measurement process. As the substrate used is thin, over applying force during tightening up the connection might damage the circuit and hence might lead to improper connection.

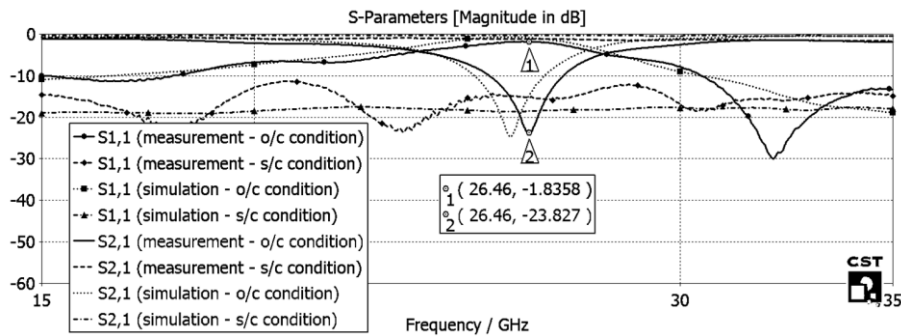


Figure 9. Simulation and measurement results of return loss (S11) and attenuation/insertion loss (S21) of the ideal switchable DGS filter using Uneven U-shape Dumbbell with open circuit (o/c) and short circuit (s/c) conditions

Figure 10 shows simulation and measurement results of ideal switchable DGS filter using the T-shape Loaded layout. Observed result of the open circuit condition filter shows similar results as the previous DGS layout, but with narrower bandwidth of attenuation response approximately 0.21 GHz at 10 dB level.

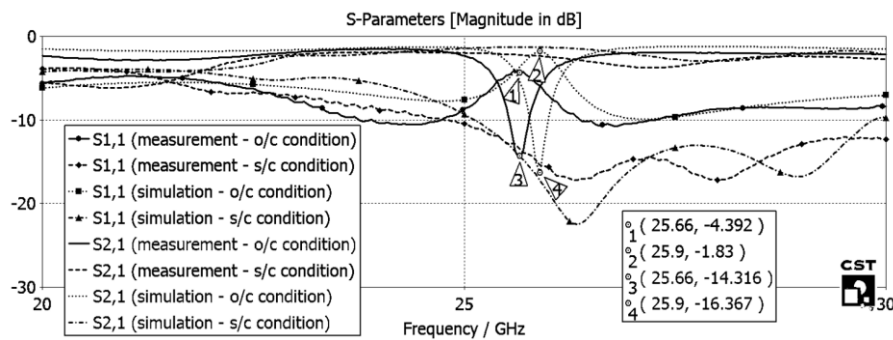


Figure 10. Simulation and measurement results of return loss (S11) and attenuation/insertion loss (S21) of the ideal switchable DGS filter using T-shape Loaded with open circuit (o/c) and short circuit (s/c) conditions

Meanwhile, short circuit condition filter also produces a wideband allpass response with an insertion loss of approximately 1.8 dB and a return loss less than 10 dB. Measurement results also have a slight shift from the simulation due to fabrication tolerance development. There is less ripple in the measurement result, which indicates good practice of measurement setup has been done.

## 5. CONCLUSION

The experimental work has successfully proved that the reconfigurable filter with DGS can interchange between bandstop and allpass responses by using open circuit and short circuit conditions of ideal switch. A good agreement between simulated and measured results was obtained for both DGSs during bandstop response with narrowband properties and also for allpass response with wideband properties in the

26 GHz band. Hence, a next future work is needed by replacing the ideal switch on the DGS with actual switching elements such as PIN diode for the actual circuit design.

## ACKNOWLEDGEMENTS

The authors would like to acknowledge the support of Center for Research and Innovation Management (CRIM), UTeM and also Akmal Danial bin Muhammad Basha and Muhammad Irsyad bin Hamzah (UTeM undergraduate students) for the research work. Appreciation towards Kementerian Pengajian Tinggi Malaysia (KPTM) for sponsoring the PhD study under Skim Latihan Akademik Bumiputra (SLAB). This study is funded by the Ministry of Higher Education (MoHE) Malaysia under Fundamental Research Grant Scheme Vot No. FRGS/1/2021/TK0/UTEM/02/8.

## REFERENCES




- [1] D. Choudhury, "5G wireless and millimeter wave technology evolution: An overview," in *2015 IEEE MTT-S International Microwave Symposium*, May 2015, pp. 1–4, doi: 10.1109/MWSYM.2015.7167093.
- [2] Y. Cho, H. K. Kim, M. Nekovee, and H. S. Jo, "Coexistence of 5G with satellite services in the millimeter-wave band," *IEEE Access*, vol. 8, pp. 163618–163636, 2020, doi: 10.1109/ACCESS.2020.3022044.
- [3] M. M. Saleh, A. A. Abbas, and A. Hammoodi, "5G cognitive radio system design with new algorithm asynchronous spectrum sensing," *Bulletin of Electrical Engineering and Informatics*, vol. 10, no. 4, pp. 2046–2054, Aug. 2021, doi: 10.11591/EEI.V10I4.2839.
- [4] O. H. Toma and M. Lopez-Benitez, "Cooperative Spectrum sensing: a new approach for minimum interference and maximum utilisation," in *2021 IEEE International Conference on Communications Workshops, ICC Workshops 2021 - Proceedings*, Jun. 2021, pp. 1–6, doi: 10.1109/ICCVWorkshops50388.2021.9473716.
- [5] P. T. Tin, D. H. Ha, P. M. Quang, N. T. Binh, and N. L. Nhat, "Performance of multi-hop cognitive MIMO relaying networks with joint constraint of intercept probability and limited interference," *Telkomnika (Telecommunication Computing Electronics and Control)*, vol. 19, no. 1, pp. 44–50, Feb. 2021, doi: 10.12928/TELKOMNIKA.V19I1.18006.
- [6] S. S. Sarma and R. Hazra, "Interference mitigation methods for D2D communication in 5G network," in *Advances in Intelligent Systems and Computing*, vol. 1040, 2020, pp. 521–530.
- [7] D. Siafarikas, E. A. Alwan, and J. L. Volakis, "Interference mitigation for 5G millimeter-wave communications," in *2018 IEEE Antennas and Propagation Society International Symposium and USNC/URSI National Radio Science Meeting, APSURSI 2018 - Proceedings*, Jul. 2018, pp. 391–392, doi: 10.1109/APUSNCURSINRSM.2018.8609455.
- [8] H. Islam, S. Das, T. Bose, and T. Ali, "Diode based reconfigurable microwave filters for cognitive radio applications: A review," *IEEE Access*, vol. 8, pp. 185429–185444, 2020, doi: 10.1109/ACCESS.2020.3030020.
- [9] A. El Fatimi, S. Bri, and A. Saadi, "Reconfigurable ultra wideband to narrowband antenna for cognitive radio applications using PIN diode," *Telkomnika (Telecommunication Computing Electronics and Control)*, vol. 18, no. 6, pp. 2807–2814, Dec. 2020, doi: 10.12928/TELKOMNIKA.v18i6.16242.
- [10] S. Narayana and Y. K. Singh, "Dual-band bandpass to bandstop switchable filter with independently tunable center frequency and bandwidth," *Microwave and Optical Technology Letters*, vol. 63, no. 11, pp. 2704–2709, Nov. 2021, doi: 10.1002/mop.32939.
- [11] S. Kingsly, M. Kanagasabai, M. G. N. Alsath, S. Subbaraj, S. K. Palaniswamy, and B. Bhuvaneshwari, "Switchable Resonator based reconfigurable bandpass/bandstop microstrip filter," *International Journal of Electronics*, vol. 108, no. 9, pp. 1610–1622, Sep. 2021, doi: 10.1080/00207217.2021.1908613.
- [12] M. K. Zahari, B. H. Ahmad, and N. A. Shairi, "Comparison of electronically switchable high Q Bandstop to bandpass filters based on allpass network," in *IEEE Symposium on Wireless Technology and Applications, ISWTA*, Aug. 2021, vol. 2021-August, pp. 43–47, doi: 10.1109/ISWTA52208.2021.9587368.
- [13] Y. Zhu and Y. Dong, "Novel dual-band bandpass-to-bandstop filter using shunt PIN switches loaded on the transmission line," in *IEEE MTT-S International Microwave Symposium Digest*, Aug. 2020, vol. 2020-August, pp. 924–927, doi: 10.1109/IMS30576.2020.9223857.
- [14] R. Chen, Q. Zhang, L. Zhou, and C. Chen, "Reconfigurable dual-band bandpass-to-bandstop filter using SAW resonators and lumped elements," in *2021 IEEE MTT-S International Wireless Symposium, IWS 2021 - Proceedings*, May 2021, pp. 1–3, doi: 10.1109/IWS52775.2021.9499428.
- [15] A. A. Zolkefli *et al.*, "Switchable bandstop to allpass filter using cascaded transmission line SIW resonators in K-band," *Bulletin of Electrical Engineering and Informatics*, vol. 10, no. 5, pp. 2617–2626, Oct. 2021, doi: 10.11591/eei.v10i5.2835.
- [16] D. Psychogiou, "Reconfigurable All-pass-to-bandstop acoustic-wave-lumped-element resonator filters," *IEEE Microwave and Wireless Components Letters*, vol. 30, no. 8, pp. 745–748, Aug. 2020, doi: 10.1109/LMWC.2020.3004028.
- [17] A. A. Bakhit and P. W. Wong, "Switchable microwave band-stop to all pass filter using stepped impedance resonator," *Progress In Electromagnetics Research B*, vol. 52, no. 52, pp. 99–115, 2013, doi: 10.2528/PIERB13033102.
- [18] W. Yang, M. D. Hickle, D. Psychogiou, and D. Peroulis, "L-band high-Q tunable quasi-absorptive bandstop-to-all-pass filter," in *IEEE MTT-S International Microwave Symposium Digest*, Jun. 2017, pp. 271–273, doi: 10.1109/MWSYM.2017.8059094.
- [19] A. C. Guyette, E. J. Naglich, and S. Shin, "Switched allpass-to-bandstop absorptive filters with constant group delay," *IEEE Transactions on Microwave Theory and Techniques*, vol. 64, no. 8, pp. 2590–2595, Aug. 2016, doi: 10.1109/TMTT.2016.2586054.
- [20] S. M. Shah *et al.*, "A 2.45 GHz microstrip antenna with harmonics suppression capability by using defected ground structure," *Bulletin of Electrical Engineering and Informatics*, vol. 9, no. 1, pp. 387–395, Feb. 2020, doi: 10.11591/eei.v9i1.1847.
- [21] W. A. Awan, S. I. Naqvi, A. H. Naqvi, S. M. Abbas, A. Zaidi, and N. Hussain, "Design and characterization of wideband printed antenna based on DGS for 28 GHz 5G applications," *Journal of Electromagnetic Engineering and Science*, vol. 21, no. 3, pp. 177–183, Jul. 2021, doi: 10.26866/jees.2021.3.r.24.
- [22] N. Muchhal, A. Chakraborty, T. Agrawal, and S. Srivastava, "Miniaturized and Selective half-mode substrate integrated waveguide bandpass filter using hilbert fractal for Sub-6 GHz 5G applications," *IETE Journal of Research*, pp. 1–8, Jan. 2022, doi: 10.1080/03772063.2021.2021816.






- [23] G. Soundarya and N. Gunavathi, "Compact dual-band SIW band pass filter using CSRR and DGS structure resonators," *Progress in Electromagnetics Research Letters*, vol. 101, pp. 79–87, 2021, doi: 10.2528/PIERL21091301.
- [24] V. Komarov, O. Barybin, and Y. V. Rassokhina, "Low-pass load matching network design using dumbbell-shaped DGS for high-efficiency microwave power amplifiers," in *2019 International Conference on Information and Telecommunication Technologies and Radio Electronics, UkrMiCo 2019 - Proceedings*, Sep. 2019, pp. 1–4, doi: 10.1109/UkrMiCo47782.2019.9165469.
- [25] A. Khare, S. Kharat, A. Rajapkar, S. M. Rathod, and M. Kulkarni, "Design of a compact wilkinson power divider using four asymmetric DGS for harmonic suppression," in *Proceedings of the 2019 TEQIP - III Sponsored International Conference on Microwave Integrated Circuits, Photonics and Wireless Networks, IMICPW 2019*, May 2019, pp. 353–356, doi: 10.1109/IMICPW.2019.8933177.
- [26] A. Amir, M. Ashkan, S. Sadegh, and M. Khalil, "A Novel Compact Reconfigurable Defected Ground Structure Resonator on Microstrip Technology for Filter Applications," in *21th Iranian Conference on Electric Engineering*, 2013, pp. 1–5, [Online]. Available: <https://civilica.com/doc/208653/certificate/print/%0Ahttps://civilica.com/doc/208653/>.
- [27] H. A. Mohamed, H. B. El-Shaarawy, E. A. F. Abdallah, and H. M. El-Hennawy, "Frequency-reconfigurable microstrip filter with dual-mode resonators using RF PIN diodes and DGS," *International Journal of Microwave and Wireless Technologies*, vol. 7, no. 6, pp. 661–669, Dec. 2015, doi: 10.1017/S1759078714001032.
- [28] A. Othman *et al.*, "Switchable open loop square ring dgs in millimeter-wave SPDT discrete switch design," in *2021 IEEE Asia-Pacific Conference on Applied Electromagnetics, APACE 2021*, Dec. 2021, pp. 1–4, doi: 10.1109/APACE53143.2021.9760600.
- [29] A. Othman *et al.*, "Millimeter-wave SPDT Discrete switch design with reconfigurable circle loaded dumbbell DGS," in *2022 International Workshop on Antenna Technology (iWAT)*, May 2022, pp. 49–52, doi: 10.1109/iWAT54881.2022.9811052.
- [30] L. H. Weng, Y. C. Guo, X. W. Shi, and X. Q. Chen, "An overview on defected ground structure," *Progress In Electromagnetics Research B*, vol. 7, pp. 173–189, 2008, doi: 10.2528/pierb08031401.

## BIOGRAPHIES OF AUTHORS






**Adib Othman**    was born in Malaysia in 1986. He is a PhD candidate from Universiti Tun Hussein Onn Malaysia. He received the Bachelor of Engineering (Hons) Electrical from Universiti Teknologi MARA in the year 2009. In 2015, he obtained his Master of Electrical Engineering in the field of Electromagnetic Compatibility from Universiti Tun Hussein Onn Malaysia. From 2015 to 2020, he was a lecturer at Fakulti Teknologi Kejuruteraan Elektrik dan Elektronik (FTKEE), Universiti Teknikal Malaysia Melaka (UTeM), Malaysia. His research interests are mainly focused on RF and Microwave Engineering. He can be contacted at email: [adib@utem.edu.my](mailto:adib@utem.edu.my).






**Noor Azwan Shairi**    was born in Malaysia. He received the Bachelor in Engineering (Electrical-Telecommunication) and the Master in Electrical Engineering from Universiti Teknologi Malaysia (UTM), in 2002 and 2005, respectively. In 2015, he obtained his Ph.D. degrees from Universiti Teknikal Malaysia Melaka (UTeM) in the field of Electronic Engineering (RF and Microwave). He is currently a Senior Lecturer at the Fakulti Kejuruteraan Elektronik dan Kejuruteraan Komputer (FKEKK), Universiti Teknikal Malaysia Melaka (UTeM), Malaysia. His research interests are RF switches, switchable/tunable filters, microwave sensors, antennas & resonators. He can be contacted at email: [noorazwan@utem.edu.my](mailto:noorazwan@utem.edu.my).






**Huda A. Majid**    received the Ph.D. degree in electrical engineering from the Universiti Teknologi Malaysia (UTM). He worked as a Postdoctoral Fellow with UTM for a period of one year. He is currently a Senior Lecturer with the Faculty Engineering Technology, Universiti Tun Hussein Onn Malaysia (UTHM), Johor, Malaysia. He has published over 100 articles in journals and conference papers. His research interests include planar and flexible antennas, array antennas, reconfigurable antennas, metamaterial, and RF microwave and mm-wave devices. He can be contacted at email: [mhuda@uthm.edu.my](mailto:mhuda@uthm.edu.my).






**Zahriladha Zakaria**    was born in Johor, Malaysia. He received the B. Eng. and M. Eng. in Electrical and Electronic Engineering from the Universiti Teknologi Malaysia in 1998 and 2004 respectively, and the PhD degree in Electrical & Electronic Engineering from the Institute of Microwaves and Photonics (IMP), University of Leeds, United Kingdom in 2010. From 1998 to 2002, he was with STMicroelectronics, Malaysia where he worked as Product Engineer. He is currently a Professor at Faculty of Electronic & Computer Engineering, University Teknikal Malaysia Melaka (UTeM). He can be contacted at email: zahriladha@utem.edu.my.






**Imran Mohd Ibrahim**    is Senior Lecturer at Universiti Teknikal Malaysia Melaka and now serve as Head of Microwave Research Group. He received his bachelor, master and doctoral degree from Universiti Teknologi Malaysia, all in electrical engineering, in 2000, 2005, and 2016, respectively. He served as faculty's first Deputy Dean (Research and Post Graduate Study) and contributed to the early development of research activities at faculty and institution. He has lead several grants from industry, government and university in antenna research and wireless communication. He is also a committee member to draft the Technical Code in 5G Safety Radiation to Malaysia Technical Standard Forum Berhad. He can be contacted at email: imranibrahim@utem.edu.my.



**Mohd Haizal Jamaluddin**    received bachelor's and master's degrees in electrical engineering from Universiti Teknologi Malaysia, Malaysia, in 2003 and 2006, respectively, and the Ph.D. degree in signal processing and telecommunications from the Université de Rennes 1, France, in 2009, with a focus on microwave communication systems, especially antennas such as dielectric resonator, reflectarray and dielectric dome antennas. He is currently an Associate Professor with the Wireless Communication Centre, Faculty of Electrical Engineering, Universiti Teknologi Malaysia. His research interests include dielectric resonator antennas, printed microstrip antennas, MIMO antennas and DRA reflectarray antennas. He can be contacted at email: haizal@utm.edu.my.



**Anwar Faizd Osman**    was born in Georgetown, Penang. He received his BSc degree in Electrical Engineering from Purdue University, USA in 2003, and MSc degree in Electrical and Electronic Engineering from Universiti Sains Malaysia (USM) in 2015. His master thesis is on wideband Low Noise Amplifier design. He has published multiple technical papers on LNA, RF switches and and RF filter designs. His current role is as Engineering Manager with a Multi-national Company. His expertise includes wireless testing for mobile operators and interference hunting. He has been a committee member of IEEE ED/MTT/SSC Penang Chapter since 2015, currently serves as the chapter auditor. He is also a former deputy chair of IEEE Microwave, Electron Devices and Solid-state symposium IMESS 2018. He is part of National 5G taskforce member, Chairman of the 5G Ecosystem and Timeline sub-working group, under the Spectrum Working group of the task force. He is also leading the study on the 5G and FSS co-existence in the 5G taskforce, as well as one of the authors of the Taskforce 5G C-band report and 5G mmWave report. He can be contacted at email: anwarfaizd.osman@rhode-schwarz.com.